Energy 348 (2026) 140561

Contents lists available at ScienceDirect

Energy

journal homepage: www.elsevier.com/locate/energy

Experimental comparison of the electrical efficiency of photovoltaics and photovoltaics-thermal hybrid system in real operation conditions

Danijela Kardaš Ančić [a,*], Mirko Komatina [b], Petar Gvero [a], Bojan Knežević [a], Milan Pupčević [a]

[a] University of Banja Luka, Faculty of Mechanical Engineering, Bosnia and Herzegovina
[b] University of Belgrade, Faculty of Mechanical Engineering, Serbia

ARTICLE INFO

Keywords:
Photovoltaic-thermal system
Photovoltaic
Variable mass flow
Electrical efficiency
Thermal energy storage

ABSTRACT

This study presents an experimental investigation of the electrical performance of a conventional photovoltaic (PV) panel and a photovoltaic–thermal (PVT) hybrid system under real meteorological conditions in Bosnia and Herzegovina. The impact of varying water mass flow rates (0.017–0.067 kg/s) through a carbon steel heat exchanger on the PVT panel temperature, electrical efficiency, power output, thermal efficiency, and thermal energy storage (TES) was analyzed, with ambient temperature, solar irradiance, and wind speed recorded throughout the experiments. Experiments conducted in July demonstrated that the PVT system consistently maintained lower operating temperatures (maximum 48.86 °C) compared to the reference PV panel (maximum 61.22 °C), resulting in improved electrical efficiency and reduced temperature-related losses. The PVT system exhibited higher electrical efficiency than the reference PV panel, with efficiency improvements ranging from 4.2 % at the lowest mass flow rate (0.017 kg/s) to 7.1 % at the highest flow rate (0.067 kg/s). At this highest flow rate, the PVT system achieved its best overall performance, with an electrical efficiency of 16.21 %, an average electrical power output of 73.01 W, a daily TES temperature rise of 6.6 °C, and a thermal efficiency of 41.46 %. These results confirm that enhanced heat removal directly supports improved photovoltaic performance and demonstrate that appropriate thermal management enables simultaneous improvement of electrical and thermal energy conversion, highlighting the potential of low-cost carbon steel heat exchangers for practical and efficient PVT operation under real operating conditions.

1. Introduction

Renewable energy systems play a crucial role in the energy sector by enhancing energy security, reducing costs and emissions, promoting sustainability, and stimulating economic growth and employment through industrial development [1]. According to the International Energy Agency (IEA), renewable energy sources are expected to surpass coal as the dominant source of electricity generation in the near future, while photovoltaic (PV) technology is projected to exceed nuclear power generation [2]. These trends emphasize the growing importance of PV technology as one of the key energy technologies of the future. Although PV systems are the most widespread technology for harnessing solar energy, their performance is strongly influenced by environmental factors, including solar irradiance, wind speed, ambient temperature, dust accumulation, soiling, and shading [3–7].

In a comprehensive review study [8] examining factors affecting PV panel performance, the authors reported that approximately 50 % of the analyzed studies focused on the impact of environmental conditions. These conclusions emphasize the importance of analyzing environmental factors when evaluating PV system performance.

Typically, only a small part of the incident solar radiation on a PV panel is converted into electrical energy, with the majority is converted into heat. Depending on the materials, technical specifications, and operating conditions, PV panels generally convert up to 25 % of total solar radiation into electrical energy, while the remainder manifests as thermal energy [9–13]. The accumulation of heat within the PV panel leads to an increase in its temperature, which negatively affects electrical efficiency.The decline in electrical efficiency at elevated temperatures is primarily attributed to the reduction in open-circuit voltage (Voc). Higher temperatures increase carrier recombination and

This article is part of a special issue entitled: EGY_AESMT'25 - Invitation Only published in Energy.

* Corresponding author.
E-mail address: danijela.kardas@mf.unibl.org (D. Kardaš Ančić).

https://doi.org/10.1016/j.energy.2026.140561
Received 29 October 2025; Received in revised form 6 February 2026; Accepted 23 February 2026
Available online 24 February 2026

electron–hole pair activity, resulting in a decreased output voltage [14,15]. Additionally, higher temperatures increase the internal resistances within the cell, reducing the fill factor (FF) and further decreasing efficiency [16,17]. Empirical studies have demonstrated that the electrical efficiency of PV cells begins to decrease when the temperature exceeds 25 °C, with an approximate efficiency loss of 0.5 % for every 1 °C increase above this threshold [18–21]. Understanding and analyzing this temperature-dependent behavior is essential for optimizing PV system performance and implementing effective cooling mechanisms [22].

To mitigate temperature-induced efficiency losses, cooling techniques are required to regulate the thermal conditions of PV panels, thereby improving their electrical output. This is commonly achieved through the integration of heat exchangers combined with circulating cooling fluids, which serve to remove heat while enabling thermal energy recovery. Combining photovoltaic and thermal energy conversion within a single unit gives rise to hybrid photovoltaic-thermal (PVT) systems. Compared to conventional PV systems, PVT configurations offer multiple advantages, including cogeneration of electrical and thermal energy, reduced installation area, shorter payback periods, and overall higher energy efficiency. Studies indicate that PVT systems can deliver up to 30 % greater energy output than separate PV and solar thermal collectors occupying the same area [23]. Economic analyses further suggest that rising energy prices enhance the cost-effectiveness of PVT systems due to their dual-energy production capabilities [24]. One of the promising applications of PVT technology lies in its integration with heat pump systems for heating, cooling, solar hot water (SHW) production, where it has been shown to achieve primary energy savings of up to 36 % [25,26]. Such synergistic solutions position PVT systems as a key technology for efficient and sustainable energy utilization. Overall, existing studies show that PVT electrical and thermal performance depends on the combined effects of heat exchanger material, geometry, working fluid, and operating conditions. Although many investigations report efficiency gains using optimized designs and high-conductivity materials, most focus on laboratory-scale systems and neglect practical constraints such as material availability, manufacturability, and regional economic context. This underscores the need for experimental studies that emphasize realistic system configurations and context-specific performance evaluation.

Nomenclature		Subscripts	
t	Temperature (°C)	a	Air
Δt	Temperature difference (°C)	c	Cell
t_a	External air temperature (°C)	m	Modul
v	Wind (air) speed (m/s)	STC	Standard test conditions
G	Incident irradiance (W/m^2)	el	Electrical
c	water specific heat capacity (kJ/kg°C)	th	Thermal
A	panel surface area (m^2)	PVT	Photovoltaic-thermal
$\dot{m}$	mass flow rate (kg/s)	PV	Photovoltaic
m	water mass in TES (kg)	ref	Reference
Q	thermal energy (W)	ave	Average
I	electrical current (A)	**Abbreviation**	
V	electrical voltage (V)	PV	Photovoltaic
P	electrical power (W)	PVT	Photovoltaic-thermal
u	standard uncertainty	TES	Thermal Energy Storage
k	coverage factor	FF	Fill factor
U	expanded uncertainty	IEA	International Energy Agency

(continued on next column)

(continued)

Nomenclature		Subscripts	
Greek symbols		SHW	Solar hot water
β	Temperature coefficient (K^{-1})	LPM	Liter per minute
γ	Solar radiation coefficient (−)	CFD	Computational fluid dynamics
η_{el}	Electrical efficiency (−)	GUM	Guide to the Expression of Uncertainty in Measurement
η_{th}	Thermal efficiency (−)		

1.1. Literature review

Photovoltaic-thermal systems represent a rapidly advancing field, with ongoing research focusing both on novel design innovations and comprehensive evaluations of existing models under diverse environmental conditions. Improving the electrical efficiency of PVT systems, alongside their thermal performance, remains a key focus, particularly through optimization of heat exchanger designs and fluid flow parameters under different environmental conditions. The following section reviews the existing literature with a focus on heat exchanger materials, working fluids, flow rates, and heat exchanger designs. Key findings from experimental, numerical, and comparative studies are highlighted to identify research gaps and guide further investigation.

In [27], a copper serpentine water heat exchanger was experimentally investigated, with both energy and exergy performance analyzed under varying water flow rates. The PVT configuration exhibited higher electrical efficiency than a standard PV panel, achieving peak performance at a flow rate of 4 LPM. Another experimental investigation [28] explored spiral-shaped water heat exchangers with circular and rectangular geometries at flow rates between 0.03 and 0.06 kg/s. Results indicated that the spiral rectangular heat exchanger yielded better thermal and electrical efficiencies, with the maximum electrical efficiency at 0.06 kg/s. A comparative analysis [29] evaluated the electrical output of PV and PVT systems using a stainless steel heat exchanger with a rectangular pipe and direct-flow configuration, confirming higher power output from the PVT system. In China, aluminum heat exchangers based on water tubes and microchannels were compared [9], with the water-tube design demonstrating superior performance. In Malaysia [10], rectangular and round hollow stainless-steel tubes were tested at mass flow rates ranging from 0.01 to 0.05 kg/s, with system efficiency examined under controlled laboratory conditions. The study highlighted that increasing mass flow rates from 0.01 to 0.05 kg/s reduced the panel temperature. Spiral tube designs demonstrated the highest electrical efficiency. In Ref. [30], a trapezoidal plate heat exchanger demonstrated better overall performance compared to a plain plate, with lower exergy destruction, shorter energy payback, and higher CO_2 mitigation.

In [11], experimental testing and computational fluid dynamics (CFD) modeling of a water-cooled PVT system were combined, showing good agreement between numerical and experimental results and higher efficiency than the reference PV panel. In a study conducted in western China [31], two aluminum heat exchanger designs—a conventional harp channel and a grid channel—were compared using TRNSYS simulations and experimental testing, with the grid-channel configuration exhibiting improved thermal and electrical efficiency. In Ref. [32], a copper pipe heat exchangers integrated into a water-cooled PVT system were evaluated at flow rates from 2 to 6 LPM, demonstrating that higher water flow rates reduced PV cell temperatures and improved system performance. Numerical studies [33] compared the electrical performance of PVT systems with heat exchangers featuring serial, parallel, and biomimetic channel geometries. Among these configurations, the biomimetic heat exchanger delivered the highest electrical efficiency (14.5 %), followed closely by the parallel (14.4 %) and serial (14.3 %) designs.

Three cooling systems employing copper, aluminum, and stainless steel heat exchangers were compared in Ref. [34], showing that the copper serpentine-tube configuration provided the highest electrical output, with an increase of 16.04 %. Another comparative study [35] reported overall efficiencies of 41.244 % (copper), 40.526 % (aluminum), and 40.234 % (stainless steel). A study [36] highlighted aluminum's cost-effectiveness, achieving the shortest payback and highest annual savings.

Despite the diversity of heat exchanger designs and materials investigated, a common trend emerges across the literature: increasing coolant flow rate generally leads to reduced PV cell temperature and improved electrical efficiency, while resulting in a lower temperature increase per unit mass of the working fluid. At the same time, most comparative studies prioritize maximizing efficiency through advanced geometries or high-performance materials, while less attention is given to system simplicity, scalability, and the feasibility of fabrication using conventional industrial processes. Experiments with water/magnetite nanofluid in copper heat exchangers showed the highest energy and electrical efficiency with eight-finned tubes [37]. Review studies [38] summarized air- and water-based PVT systems, showing electrical efficiencies of 4–24 % and 5.1–15.8 %, and thermal efficiencies of 27–87 %, with honeycomb plates favorable for air-based and parallel rectangular tubes for water-based systems. A study in Ref. [39] using a grooved helical microchannel with Fe_3O_4 nanofluid reported the staggered grooved unit achieved the highest energy and exergy efficiency.

In summary, existing studies convincingly demonstrate the technical potential of PVT systems to enhance overall solar energy utilization. However, the literature remains largely centered on high-performance materials and optimized configurations, often neglecting the challenges associated with cost, local manufacturing capabilities, and large-scale deployment. Consequently, there is a lack of experimental data that establish realistic performance benchmarks for PVT systems based on widely available, low-cost materials operating under real outdoor conditions.

1.2. Research gap and study motivation

While copper and aluminum are widely investigated in photovoltaic–thermal (PVT) systems, and stainless steel is occasionally considered, the performance of conventional carbon steel as a heat exchanger material remains largely unexplored. In addition, PVT system performance is strongly influenced by geographical location and climatic conditions. Accordingly, the primary motivation of this study is to provide original, location-specific experimental data and to assess the real-world feasibility of PVT technology under the climatic conditions of Bosnia and Herzegovina. To the authors' knowledge, this is the first experimental PVT study conducted in Bosnia and Herzegovina that explicitly accounts for local climate and operating conditions.

Carbon steel was deliberately selected as a low-cost and widely available material to establish a realistic lower-bound performance benchmark for PVT systems. This approach enables clearer assessment of material-dependent thermal limitations under practical conditions. Carbon steel is particularly relevant for industrial and rural applications, where robustness, weldability, availability, and cost often outweigh marginal gains in thermal performance. In contrast, many existing studies focus on high-performance materials and optimized laboratory-scale designs, often without considering material availability, manufacturability, or regional supply chains. Such factors can significantly constrain the feasibility and large-scale deployment of PVT systems. The selection of carbon steel is also motivated by the industrial context of Bosnia and Herzegovina, where the iron and steel sector plays a key economic role. In 2024, industrial electricity consumption accounted for 23 % of total national electricity use, with the iron and steel industry representing the largest share at 18.8 % [40]. In this context, evaluating carbon steel as a PVT heat exchanger material aligns with the country's existing industrial base and offers a realistic pathway toward cost-effective energy solutions.

An appropriate-technology approach is therefore adopted, focusing on a heat exchanger design that can be manufactured, installed, and maintained using locally available resources. Although carbon steel exhibits lower thermal conductivity than copper or aluminum and may be susceptible to corrosion, its affordability and accessibility make it suitable for cost-sensitive applications. Issues related to long-term durability and corrosion mitigation are acknowledged and will be addressed in future work.

The main objective of this study is to experimentally evaluate the electrical performance of a PVT system equipped with a carbon steel heat exchanger and coupled with thermal energy storage (TES), and to analyze the influence of water mass flow rate on panel temperature, thermal storage behavior, and electrical output under real operating conditions. By addressing these aspects, the study contributes practical, application-oriented performance data and emphasizes scalability and manufacturability, supporting the deployment of PVT systems in regions with similar economic, industrial, and climatic constraints.

2. Materials and methods

2.1. Basic equations

The operating temperature of a photovoltaic cell plays a critical role in determining its electrical efficiency [41]. Numerous empirical correlations have been developed to estimate the PV cell temperature (t_c) as a function of key meteorological variables, including ambient temperature (t_a), solar irradiance (G), and wind speed (v), as well as material and system-specific properties [42–46]. At high levels of solar irradiance, a temperature difference can arise between the back surface of the PV panel (t_m) and the actual cell temperature (t_c) [47]. Under a solar irradiance of 1000 W/m^2, this temperature difference typically ranges from 2 to 3 °C in flat-plate panels. However, in flat-plate configurations with thermally insulated back surfaces, the temperature differential can be considered negligible [44]. Given that the maximum average daily solar irradiance recorded at the study location is below 750 W/m^2, this temperature difference was deemed insignificant, and it was assumed that $t_c = t_m = t_{PV} = t_{PVT}$. A linear relation describing the electrical efficiency of a PV panel as a function of its operating temperature is given in Eq. (1):

$$\eta_{el} = \eta_{STC} \cdot \left[1 - \beta \cdot (t_{PVT} - t_{STC}) + \gamma \, log_{10} \, G\right] \quad (1)$$

where η_{STC} is the panel electrical efficiency at the reference temperature $t_{STC} = 25$ °C and a solar irradiance of.

1000 W/m^2 [48,49]. The temperature coefficient β and the solar radiation coefficient γ are mainly material dependent properties, with typical values of approximately 0.004 [K^{-1}] and 0.12, respectively, for crystalline silicon panels [48–50]. The last term in Eq. (1) is commonly assumed to be zero [48–50], and Eq. (1) therefore reduces to Eq. (2):

$$\eta_{el} = \eta_{STC} \cdot [1 - \beta \cdot (t_{PVT} - t_{STC})] \quad (2)$$

This equation represents the traditional linear expression for the PVT/PV electrical efficiency as a function of the panel temperature [51,52]. Thermal efficiency of a PVT panel can be expressed as Eq. (3) [53,54]:

$$\eta_{th} = \frac{\dot{m} \cdot c \cdot \Delta t}{A \cdot G} \quad (3)$$

where $\dot{m}$ is the fluid mass flow rate through the heat exchanger [kg/s], c is the specific heat capacity of water [kJ/(kg·°C)], Δt is the measured fluid temperature rise across the heat exchanger [°C], A is the collector surface area [m^2], and G is the solar irradiance [W/m^2]. The thermal energy stored in the TES is calculated via a straightforward energy balance as Eq. (4) [55,56]:

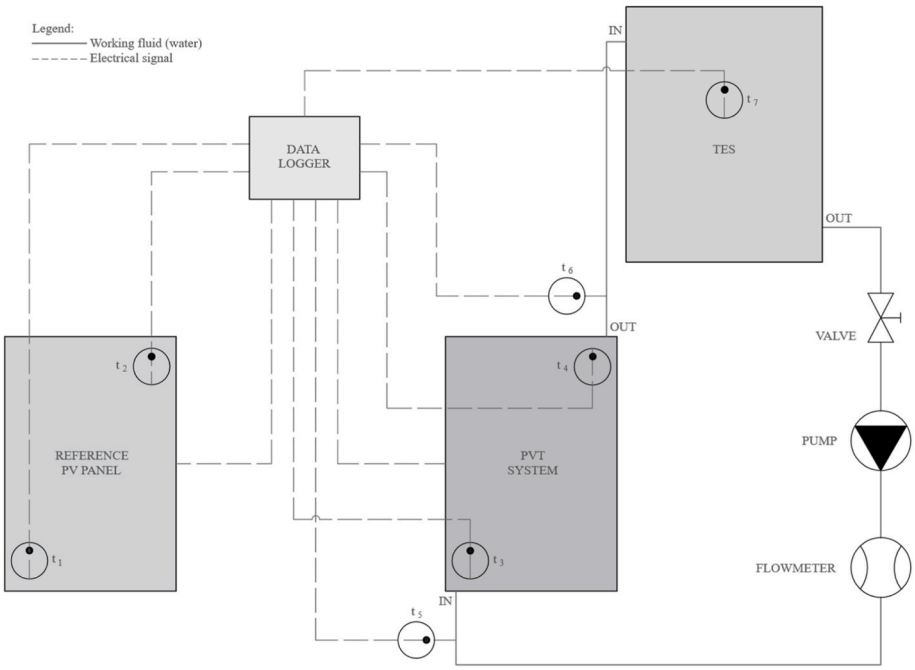

Fig. 1. Schematic of the experimental setup for analyzing the reference PV panel and PVT system integrated with a TES.

$$Q_{TES} = m \cdot c \cdot \Delta t_{TES} \quad (4)$$

Where m is water mass in the TES [kg], c is the specific heat capacity of water [kJ/kg°C], and the Δt_{TES} is the measured temperature rise in the TES.

2.2. Experimental setup and measurement procedure

As the electrical efficiency of a PV panel is highly influenced by geographic location and meteorological parameters, a experimental setup was designed, constructed, and implemented to evaluate and compare the performance of a conventional PV panel and PVT hybrid system under real operating conditions. The conventional PV panel used for comparison was of the same type as the PV panel integrated into the PVT system. This ensured that both systems shared identical PV characteristics, allowing a direct and fair comparison of their electrical performance. A schematic representation of the experimental system is shown in Fig. 1. The experimental setup was designed to enable real-time monitoring of reference PV and PVT panel temperatures, electrical current and voltage, while simultaneously recording key meteorological parameters including solar irradiance, ambient air temperature, and wind speed. These measurements were used to evaluate and compare the electrical output of the reference PV panel and the PVT hybrid system under naturally varying operating conditions, as well as to assess the thermal efficiency of the PVT system and the thermal behavior of the TES. Thermal efficiency was calculated using the gross collector area of the PVT panel as the reference area. A detailed uncertainty analysis of the measured and derived parameters (temperatures, electrical efficiency and power output) was conducted following the Guide to the Expression of Uncertainty in Measurement (GUM) approach and is presented in Section 3 (Results and Discussion) as Subsection 3.1 (Uncertainty analysis).

In the PVT configuration, a direct-flow heat exchanger was implemented using water as the working fluid (Fig. 2). The heat exchanger consisted of 12 carbon steel channels with a cross-sectional area of 20 × 20 mm, providing extensive coverage of the rear surface of the PV panel

Energy

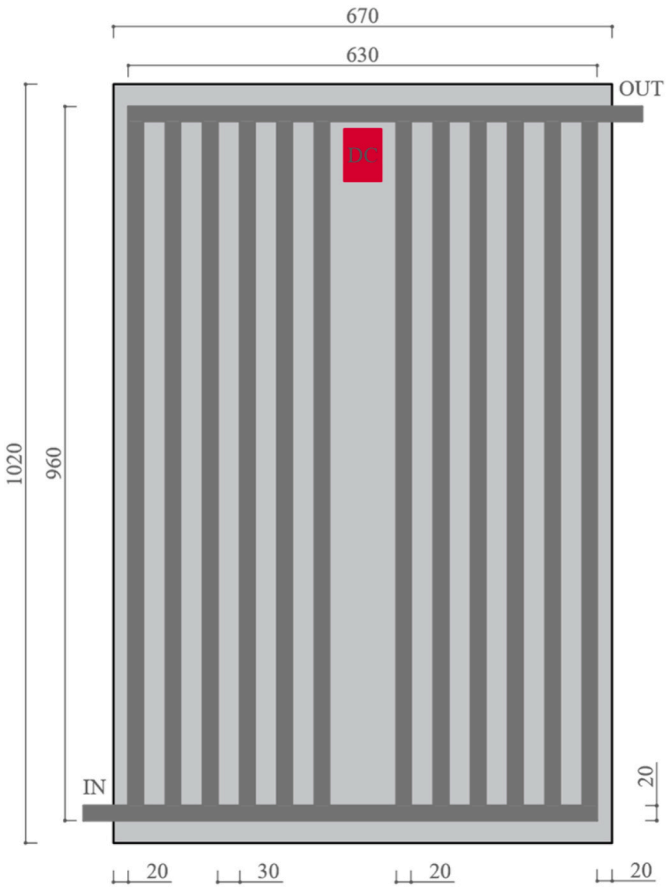

Fig. 2. Analyzed direct-flow heat exchanger.

Fig. 3. Experimental set-up (a – reference PV panel and PVT system with meteorological station; b – PVT backsurface; c – PV panel backsurface with position of PT100 temperature sensors; d – TES).

and ensuring effective heat extraction. This configuration was selected to achieve a balance between thermal performance, structural robustness, manufacturability, ease of installation, and overall cost-effectiveness, making it suitable for realistic residential, rural, and industrial applications.

An overview of the experimental installation and its main components is shown in Fig. 3. The experimental setup is located outdoors at the Faculty of Mechanical Engineering, University of Banja Luka (44.46282° N, 17.11502° E) in Bosnia and Herzegovina. Wind speed and ambient air temperature were recorded using a.

PCE-FWS20N meteorological station positioned adjacent to the test installation. Solar irradiance was recorded using the meteorological station Luft WS10 mounted on the rooftop of the same building to ensure unobstructed exposure to sunlight. The technical specifications of the PV panel and the meteorological stations employed in the study are listed in Tables 1 and 2, respectively.

Table 1
Technical specification of the PV panel.

Standard Test Conditions AM = 1.5, E = 1000 W/m^2, T_C = 25 °C	
Nominal Power	100 W
Cell Type/Efficiency	Monocrystalline/17.66 %
Maximum Power Current (I_m)	5.41 A
Maximum Power Voltage (V_m)	18.50 V
Open-circuit Voltage (V_{oc})	22.50 V
Short-circuit Current (I_{sc})	5.92 A
Working Temperature	−40 °C to +80 °C
Panel Dimensions	1020 × 670 × 35 mm

Table 2
Technical specification of the meteorological stations.

PCE - FWS20N	
Air temperature	−40 ÷ + 60 °C (±1,0 °C)
Wind speed	0 ÷ 50 m/s (±1 m/s, wind speed <5 m/s; ±10 m/s, wind speed >5 m/s)
Luft WS10	
Irradiance	Silicium - Pyranometer, 0 ÷ 1500 W/m^2 (±10 % or ±120 W/m^2)

The reference PV and PVT panel temperatures were measured using PT100 temperature sensors, positioned diagonally at the lower-left and upper-right corners (Fig. 3c), to account for possible temperature non-uniformities across the panel surfaces. The same sensor type and the same positioning strategy were applied to both systems. For subsequent analysis, the arithmetic mean of the two measured values was used as a representative panel surface temperature. The PT100 temperature sensors have a specified accuracy of $\pm(0.15 + 0.002 \times |t|)$ °C, within a temperature range of −50 °C to 300 °C. In the PVT configuration, water was used as the working fluid, circulating through a heat exchanger mounted on the rear side of the panel and hydraulically connected to a thermal energy storage (TES) unit. The TES consisted of a cylindrical 200 L water tank located indoors within the Faculty of Mechanical Engineering to simulate realistic residential or commercial operating conditions. The tank was insulated with 30 mm mineral wool to minimize heat losses. The internal heat exchanger was connected to the PVT system via 12 mm diameter water pipes, insulated with 10 mm pipe insulation, with a total pipe length of approximately 14 m.

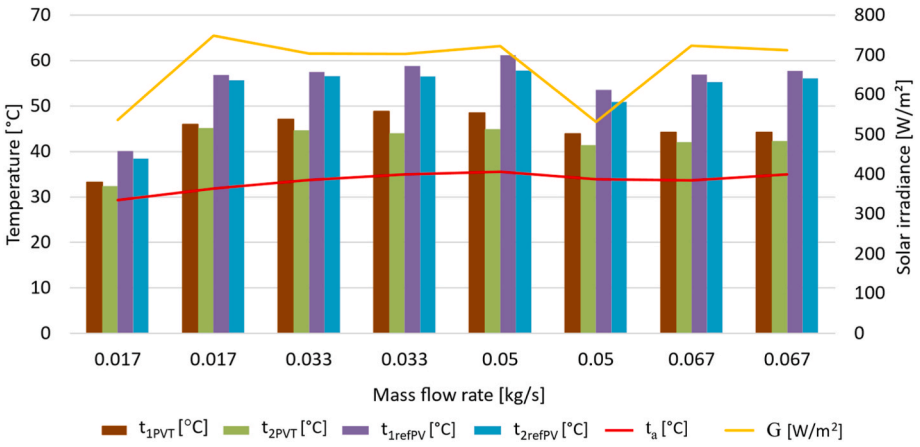

Fig. 4. Average daily temperature measurements of the reference PV panel and the PVT panel in two points (Calculated uncertainties are smaller than the symbol size and are therefore not visible in the figure).

Water temperature within the TES was measured using a Siemens QAE2111.010 immersion temperature sensor with a specified accuracy of ±0.95 °C over a temperature range from −30 °C to 130 °C. Each morning prior to system operation, the TES was filled with fresh tap water supplied directly from the municipal water network, reflecting the practical operation of real-world PVT systems. During the experimental campaign, the initial TES water temperature ranged between 22.3 °C and 24.2 °C. These variations were considered representative of normal operating conditions and were not expected to significantly influence the system-level evaluation, as the analysis focused on the daily temperature rise (Δt_{TES}) and thermal energy accumulation in the TES rather than on absolute temperature values. The experimental campaign was conducted over eight selected days in July 2024 (between July 4 and July 17), with July chosen as representative of peak summer conditions at the investigated geographic location [57]. Four different water mass flow rates were examined: 0.017 kg/s, 0.033 kg/s, 0.050 kg/s, and 0.067 kg/s. Each mass flow rate was tested over two consecutive days. This approach allowed the system performance to be evaluated under consistent operational conditions while simultaneously capturing natural day-to-day variations in meteorological parameters such as solar irradiance, ambient temperature, and wind speed. By analyzing system performance over multiple days for each operating condition, the influence of short-term weather fluctuations was preserved in the dataset, while the repetition of measurements reduced random variability and improved the reliability of the results. No artificial isolation or control of meteorological conditions was applied, as the primary objective of this study was to assess the PVT system performance under real-world, dynamically changing environmental conditions. This study prioritizes system-level realism over strict parameter isolation. All measurements were conducted daily between 10:00 and 16:00, with a data acquisition interval of 10 min, and recorded using an EASY-E4-UC-12RC1 data acquisition system. Instantaneous performance parameters were calculated at each 10-min interval, while daily average values were obtained by averaging all measurements recorded between 10:00 and 16:00 for each operating day. The selected sampling interval represents a compromise between capturing meaningful variations in system performance and avoiding unnecessary data redundancy. To provide a comprehensive overview, two-day averages were calculated for each mass flow rate analyzed by averaging the daily values over the two consecutive days.

3. Results and discussion

During the experimental campaign, the average daily solar irradiance ranged from 532 W/m^2 to 749 W/m^2, ambient air temperature ranged between 29 and 36 °C, and wind speed ranged from 0.332 m/s to 0.558 m/s. Cloudy conditions were recorded on July 4 and July 17, resulting in reduced average irradiance values of 536.35 W/m^2 and 532.31 W/m^2, respectively. On the remaining days, meteorological parameters exhibited only minor variations, allowing a consistent comparison of the reference PV and PVT systems performance under natural operating conditions.

The temperatures of the PV and PVT panels were recorded at two diagonal positions on the rear surface (lower-left and upper-right corners, Fig. 4). For both systems and on all measurement days, the upper measurement point consistently exhibited higher temperatures. This behavior may be attributed to the combined effects of natural convection, non-uniform solar irradiance distribution, partial shading caused by the panel frame, and heat dissipation through the mounting structure. In the PVT system, the upward flow of the working fluid further contributed to higher temperatures at the upper region of the panel. The maximum average daily temperature of the reference PV panel reached 61.22 °C, whereas the PVT panel exhibited a corresponding maximum average daily temperature of 48.86 °C under comparable conditions

Table 3
Average daily values of the measured parameters for each test day.

Mass flow rate [kg/s]	Date	$t_{ave\text{-}PVT}$ [°C]	$t_{ave\text{-}refPV}$ [°C]	t_a [°C]	G [W/m^2]	v [m/s]
0.017	4.7.	32.82	39.26	29.31	536.35	0.427
	5.7.	46.94	56.30	31.88	748.39	0.425
0.033	10.7.	45.90	57.03	33.75	703.21	0.351
	11.7.	46.47	57.69	34.95	702.59	0.332
0.050	16.7.	46.73	59.54	35.53	722.56	0.405
	17.7.	42.70	52.26	33.93	532.31	0.381
0.067	8.7.	43.18	56.11	33.68	722.93	0.558
	9.7	43.29	56.95	34.98	711.89	0.548

Table 4
Overall average values of the PVT temperature for each mass flow rate as well as average PVT and PV electrical efficiency.

Mass flow rate [kg/s]	$t_{ave\text{-}PVT}$ [°C]	$t_{ave\text{-}refPV}$ [°C]	Δt [°C]	$\eta_{ave\text{-}PVT}$	$\eta_{ave\text{-}refPV}$
0.017	39.88	47.78	7.90	0.1652	0.1585
0.033	46.19	57.36	11.18	0.1597	0.1509
0.050	44.72	55.90	11.19	0.1609	0.1522
0.067	43.24	56.53	13.30	0.1621	0.1515

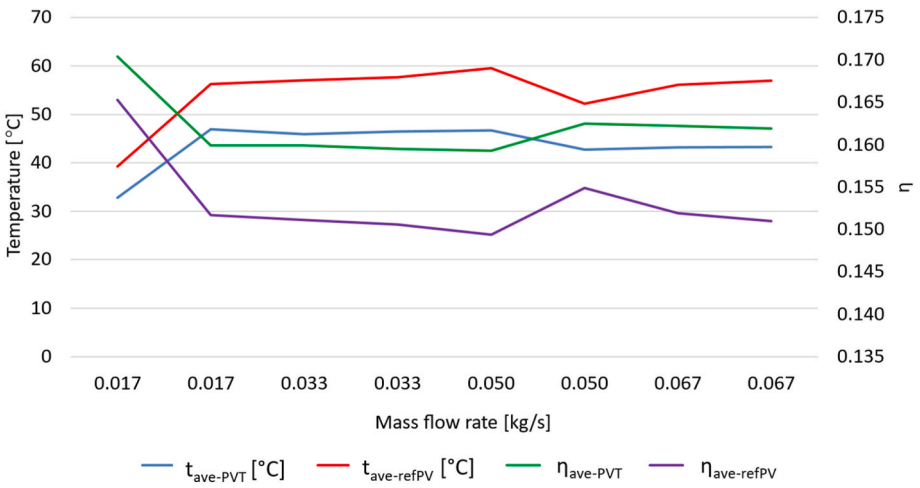

Fig. 5. Electrical efficiency of the reference PV panel and PVT hybrid system (Calculated uncertainties are smaller than the symbol size and are therefore not visible in the figure).

(Fig. 4). Table 3 summarizes the average daily temperatures of both panels for all tested mass flow rates. Across all operating conditions, the PVT panel consistently operated at lower temperatures than the reference PV panel, demonstrating the effectiveness of the integrated heat exchanger in extracting excess thermal energy from the photovoltaic panel.

Table 4 presents the average values of all measured parameters, obtained by averaging two consecutive measurement days for each mass flow rate. Over the examined mass flow rate range from 0.017 kg/s to 0.067 kg/s, the average temperature of the PVT panel remained significantly lower than that of the reference PV panel. At the lowest flow rate (0.017 kg/s), the PVT panel operated at 39.88 °C compared to 47.78 °C for the reference panel, whereas at the highest flow rate (0.067 kg/s) the temperature difference increased to 13.30 °C. These results suggest that solar irradiance and working fluid mass flow rate are the dominant factors governing panel temperature. Increasing the mass flow rate enhances convective heat removal from the PVT panel, stabilizing or reducing its operating temperature and thereby improving electrical performance. In contrast, the temperature of the reference PV panel closely followed variations in solar irradiance. Ambient air temperature also influenced panel temperatures, with higher ambient temperatures leading to increased panel temperatures. Wind speeds between 0.33 m/s and 0.56 m/s showed a limited influence on thermal performance, which may be attributed to their relatively low magnitude and the dominant role of forced convection within the PVT heat exchanger. The comparison between the lowest (0.017 kg/s) and highest (0.067 kg/s) flow rates ilustrates the combined influence of meteorological conditions, coolant residence time, and heat extraction capability. At 0.017 kg/s, favorable meteorological conditions combined with longer residence time resulted in the lowest PVT panel temperature (39.88 °C) and the highest electrical efficiency (0.1652). At intermediate flow rates, less favorable ambient conditions resulted in higher panel temperatures and reduced electrical efficiency. For the 0.033 kg/s case, lower wind speed and higher ambient temperature and irradiance led to the highest PVT panel temperature (46.19 °C) and the lowest electrical efficiency (0.1597). At 0.067 kg/s, the increased flow rate enhanced total heat removal and slightly higher wind speed reduced the PVT panel temperature to 43.24 °C, increasing the electrical efficiency to 0.1621. Although this efficiency did not exceed the maximum observed at the lowest flow rate due to shorter residence time and less favorable ambient conditions, it remained higher than that of the reference PV panel for all cases. Overall, electrical efficiency increased with enhanced heat removal and remained inversely related to panel temperature. In all cases, the PVT panel operated at significantly lower temperatures and higher electrical efficiency than the reference PV panel. These findings demonstrate the combined influence of residence time, working fluid flow rate, and meteorological conditions.

Table 5
Average output parameters of the reference PV panel and the PVT system at different working fluid mass flow rates.

Mass flow rate [kg/s]	Voltage PVT [V]	Current PVT [A]	Power output PVT [W]	Voltage refPV [V]	Current refPV [A]	Power output refPV [W]
0.017	13.06	3.99	59.07	12.46	4.09	57.50
0.033	15.11	4.70	71.36	14.96	4.74	71.26
0.050	12.86	4.33	59.50	12.70	4.37	59.23
0.067	15.80	4.61	73.01	15.39	4.64	71.53

Electrical performance followed a similar trend. As shown in Fig. 5, the PVT system exhibited higher electrical efficiency than the reference PV panel across all tested mass flow rates, with values ranging from 15.97 % to.

16.52 %, compared to 15.09 % to 15.85 % for the reference PV panel. This improvement is attributed to reduced operating temperatures of the PVT panel.

The electrical output parameters summarized in Table 5 further support these findings. Daily average electrical power was determined by averaging the instantaneous power values, calculated at each 10-min interval as the product of the measured voltage and current. Since the reported daily average voltage and current are calculated independently as arithmetic means of time-resolved measurements, the resulting average electrical power is not, in general, equal to the product of these average values.

For all examined mass flow rates, the PVT system produced equal or higher power output than the reference PV panel. At the highest flow rate of 0.067 kg/s, the PVT panel delivered a maximum average power output of.

73.01 W, compared to 71.53 W for the PV panel. At 0.033 kg/s, both systems exhibited nearly identical power output despite a higher electrical efficiency of the PVT panel. This apparent discrepancy arises because electrical efficiency is temperature-dependent, whereas absolute power output also depends on solar irradiance and panel area. In the present measurements, both the PVT and reference PV panels operated under nearly identical irradiance and area conditions, which explains the very similar power outputs. However, the PVT panel operated at a significantly lower temperature, which reduced temperature-related electrical losses, resulting in a higher electrical efficiency (PVT: 0.1597 vs. PV: = 0.1509). A similar trend is observed across all other measured flow rates, demonstrating that the higher electrical efficiency

Table 6
Daily temperature rise in the TES, the stored thermal energy, and the thermal efficiency of the PVT system for each mass flow rate.

Mass flow rate [kg/s]	Δt_{TES} [°C]	Q_{TES} [kWh]	$\eta_{th,PVT}$
0.017	5.1	1.186	0.1694
0.033	6.1	1.420	0.2984
0.050	6.2	1.444	0.4112
0.067	6.6	1.535	0.4146

of the PVT system consistently reflects improved energy conversion compared to the reference PV, despite closely matched instantaneous power outputs.

Cloudy conditions on July 4 and July 17 resulted in reduced solar irradiance, leading to lower panel temperatures and decreased thermal and electrical performance of both the PVT and reference PV systems compared to clear-sky days. Although reduced temperatures can slightly improve electrical efficiency, the limited solar input and higher share of diffuse radiation led to lower electrical power output, which is reflected in the lowest measured power values during the campaign. Data from these days were intentionally retained in the analysis to capture system behavior under realistic and dynamically varying meteorological conditions. Including such conditions provides a more representative assessment of PVT performance and highlights the sensitivity of both systems to short-term weather variability.

In addition to enhanced electrical performance, the PVT system demonstrated measurable thermal energy generation. Table 6 summarizes the daily temperature rise in the TES, the stored thermal energy, and the thermal efficiency of the PVT system for each mass flow rate. Both the TES temperature rise and the thermal efficiency increased as the mass flow rate increased, indicating improved heat extraction from the PVT panel and enhanced heat transfer to the TES.

The combined analysis of PVT thermal efficiency and TES temperature rise demonstrates the interplay between working fluid mass flow rate, panel thermal behavior, and thermal energy storage performance. As the mass flow rate increases, both the thermal efficiency of the PVT panel and the temperature rise in the TES increase overall, indicating enhanced heat extraction and transfer to the storage system. Higher flow rates allow a greater amount of thermal energy to be removed from the panel per unit time, reducing relative thermal losses and increasing the total heat delivered to the TES. At the same time, the temperature gain per unit mass of working fluid decreases at higher flow rates because the fluid residence time within the collector is reduced. As a result, the TES temperature rise (Δt) increases more moderately rather than proportionally with the thermal efficiency ($\eta_{th,PVT}$). Conversely, at lower flow rates, the working fluid remains in the collector for a longer duration, leading to a higher Δt per unit mass, while the overall thermal efficiency remains lower due to slower heat transfer and larger proportional thermal losses. Accordingly, the highest TES temperature rise, the largest amount of thermal energy stored in the TES, and the highest PVT thermal efficiency were observed at a mass flow rate of 0.067 kg/s, whereas the lowest values occurred at 0.017 kg/s. The combined consideration of $\eta_{th,PVT}$ and Δt provides a realistic system-level performance indicator, capturing not only the collector's thermal efficiency but also the actual thermal energy accumulated in the TES, including the effects of natural convection and the thermal inertia of the storage unit. These thermal performance trends are consistent with the observed reduction in reference PV and PVT panel temperatures and the corresponding improvement in PVT electrical efficiency, indicating a strong coupling between heat removal and overall PVT system performance. The results further suggest that system operation can be flexibly optimized through flow-rate control, allowing prioritization of electrical output, thermal energy production, or TES charging, depending on operational requirements. Such flexibility enhances the industrial relevance of the system and enables adaptation to variable energy demands. Fig. 6 compares the overall efficiency of the PVT system with that of the reference PV panel. The overall PVT efficiency is defined as the sum of electrical and thermal efficiencies, reflecting the system's capability to simultaneously generate electricity and recover useful thermal energy. As the water mass flow rate increases from 0.017 kg/s to 0.067 kg/s, the average PVT efficiency increases substantially from 33.45 % to 57.66 %, demonstrating the strong dependence of total system performance on heat removal capability. At lower mass flow rates, limited heat extraction constrains thermal efficiency and overall performance, whereas higher flow rates enhance convective heat transfer and thermal energy recovery. In contrast, the efficiency of the reference PV panel remains nearly constant at approximately from 15 % to 16 %, confirming that the observed improvement in overall efficiency is primarily driven by the thermal contribution of the PVT system. The consistently lower operating temperatures of the PVT panel further indicate effective thermal management, which mitigates temperature-related electrical losses while enabling substantial thermal energy harvesting. Overall, these results demonstrate that the coupled thermal and electrical operation of the PVT system enables superior solar energy utilization compared to standalone PV technology, highlighting the fundamental advantage of PVT systems under real operating conditions.

3.1. Uncertainty analysis

Measurement uncertainty was evaluated for all key experimental variables following the Guide to the Expression of Uncertainty in Measurement (GUM). Standard uncertainties (u) were evaluated as Type B contributions based on sensor specifications and equipment tolerances.

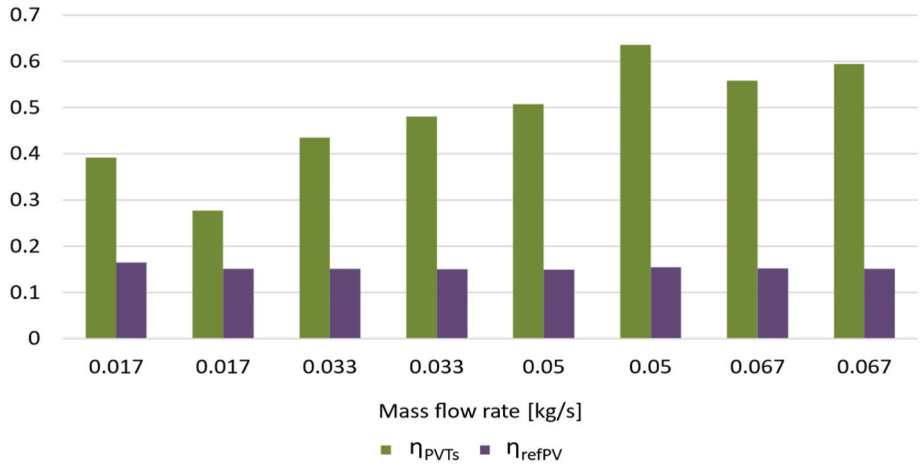

Fig. 6. Overall efficiency of the PVT system and electrical efficiency of the reference PV panel.

Table 7
Summary of sensor accuracies used in the experiments.

Sensor	Measured quantity	Accuracy
PT100 thermocouple	Panel temperature	± (0.15 + 0.002 × |t|) °C
Immerson sensor	TES temperature	±0.95 °C
Flowmeter	Mass flow rate	0.3 %
Voltage divider + PLC ADC	PV voltage V	Resistor tolerance ± 10 %, ADC 12 bit
Current transducer	PV current I	±0.75 % FSR

Independent contributions were combined using the root-sum-of-squares (RSS) method. Expanded uncertainties (U) were calculated using a coverage factor $k = 2$, corresponding to a confidence level of approximately 95 %:

$$U = k \cdot u = 2 \cdot u \tag{5}$$

Table 7 summarizes the measurement sensors used in the experiments along with their specified accuracies. These accuracies were considered for the uncertainty analysis of the measured quantities, such as panel temperatures, electrical efficiency and power of the PVT and PV systems.

The uncertainty of the measured and calculated parameters was evaluated to ensure a reliable assessment of the PVT system performance. The standard uncertainty of the mean temperature was determined by propagating the sensor accuracy:

$$u(t) = \frac{0.15 + 0.002 \cdot |t|}{\sqrt{3}}\ [^\circ\mathrm{C}];\quad U(t) = 2 \cdot u(t) \tag{6}$$

The standard uncertainty of the panel electrical efficiency, $u(\eta_{el})$, was obtained by propagating the relevant measurement uncertainties through the electrical efficiency model:

$$\eta_{el} = \eta_{STC} \cdot [1 - \beta \cdot (t_c - t_{STC})] \tag{7}$$

$$u(\eta_{el}) = \beta \cdot \eta_{STC} \cdot u(T);\quad U(\eta_{el}) = 2 \cdot u(\eta_{el}) \tag{8}$$

Instantaneous electrical power was computed as:

$$P = V \cdot I \tag{9}$$

For independent voltage V and current I measurements, the combined standard uncertainty is:

$$u(P) = \sqrt{(I \cdot u(V_{in}))^2 + (V_{in} \cdot u(I))^2};\quad U(P) = 2 \cdot u(P) \tag{10}$$

Voltage and current uncertainties were evaluated based on ADC quantization, sensor accuracy, and transfer function tolerances. The results of this uncertainty analysis for each flow rate are summarized in Table 8. This approach provides a clear quantification of the uncertainties associated with both measured temperatures and calculated electrical efficiencies, consistently accounting for instrument and sensor accuracies.

The evaluated Type B uncertainties are low and well characterized, with temperature uncertainties of.

0.13 °C to 0.15 °C, electrical efficiency uncertainties on the order of 10^{-4}, and relative output power uncertainties of approximately from 4 % to 6 %. The corresponding expanded uncertainties provide clear quantitative bounds on the measured and derived parameters, supporting the reliability of the experimental data and enabling a robust comparison between the PVT system and the reference PV panel. The magnitude of these uncertainties indicates that the observed performance differences exceed the associated measurement uncertainty.

4. Conclusion

This study presents an experimental investigation of a photovoltaic–thermal (PVT) system employing a carbon steel heat exchanger, addressing a research gap in which conventional low-cost materials have been largely overlooked in favor of copper or aluminum. Conducted in Bosnia and Herzegovina, the study provides original, location-specific experimental data and evaluates the real-world feasibility of PVT systems under local climatic conditions. The use of carbon steel - a robust, affordable, and widely available material - demonstrates that practical and cost-effective PVT solutions can be implemented without reliance on high-performance metals, particularly in industrial and rural contexts where material accessibility and manufacturing constraints are decisive.

The PVT system consistently operated at lower temperatures than the reference PV panel while maintaining higher electrical efficiency. The overall system efficiency, accounting for both electrical output and recovered thermal energy, increased from 33.45 % to 57.66 % as the water mass flow rate increased from 0.017 kg/s to 0.067 kg/s, reflecting the strong influence of heat removal on total system performance. Limited heat extraction at low flow rates constrained overall efficiency, whereas higher flow rates enhanced thermal energy recovery. In contrast, the electrical efficiency of the reference PV panel remained nearly constant at approximately from 15 % to 16 %, indicating that the improvement in overall efficiency is primarily attributable to the thermal contribution of the PVT system. At the highest flow rate, the system achieved the largest thermal energy transfer to the thermal energy storage (TES), with a thermal efficiency of 0.4146 and a TES temperature rise of 6.6 °C, while the electrical efficiency reached 16.21 %, exceeding that of the reference PV panel. The results of this study provide a realistic lower-bound performance benchmark for water-based PVT systems using low-cost and widely available heat exchanger material, rather than an optimized configuration. Although variable meteorological conditions prevent strict parameter isolation, the real-world experimental approach captures system-level behavior under practical operating conditions, which is essential for assessing feasibility and scalability. The thermal energy storage analysis and PVT thermal efficiency are included to indicate heat recovery and storage behavior at the system level, complementing the electrical performance evaluation rather than providing a detailed thermal optimization. Beyond the local context, the findings offer relevant insights for the design and scaling of PVT systems in regions with similar economic, industrial, and climatic conditions. Overall, the results demonstrate that low-cost, locally

Table 8
Type B measurement uncertainties.

Panel	t [°C]	$u(t)$	$U(t)$	η_{el}	$u(\eta_{el})$	$U(\eta_{el})$	P[W]	$u(P)$	$U(P)$
PVT	39.88	0.133	0.266	0.1652	9.37×10^{-5}	1.87×10^{-4}	59.07	2.89	5.78
PVT	46.19	0.140	0.280	0.1597	$9.87\cdot10^{-5}$	$1.97\cdot10^{-4}$	71.36	3.92	7.84
PVT	44.72	0.138	0.276	0.1609	$9.71\cdot10^{-5}$	$1.94\cdot10^{-4}$	59.50	3.08	6.15
PVT	43.24	0.137	0.274	0.1621	$9.63\cdot10^{-5}$	$1.93\cdot10^{-4}$	73.01	4.02	8.03
PV_{ref}	47.78	0.142	0.284	0.1585	$1.00\cdot10^{-4}$	$2.00\cdot10^{-4}$	57.50	2.82	5.65
PV_{ref}	57.36	0.153	0.306	0.1515	$1.08\cdot10^{-4}$	$2.16\cdot10^{-4}$	71.26	3.91	7.82
PV_{ref}	55.90	0.151	0.302	0.1522	$1.07\cdot10^{-4}$	$2.14\cdot10^{-4}$	59.23	3.07	6.14
PV_{ref}	56.53	0.152	0.304	0.1515	$1.08\cdot10^{-4}$	$2.16\cdot10^{-4}$	71.53	3.94	7.89

available materials can support manufacturable and economically viable PVT solutions, bridging the gap between laboratory studies and real-world deployment.

CRediT authorship contribution statement

Danijela Kardaš Ančić: Writing – original draft, Methodology, Investigation, Formal analysis, Conceptualization. **Mirko Komatina:** Writing – review & editing, Supervision, Methodology. **Petar Gvero:** Writing – review & editing, Resources. **Bojan Knežević:** Investigation, Conceptualization. **Milan Pupčević:** Investigation, Conceptualization.

Disclaimer

Funded by the European Union. Views and opinions expressed are however those of the author(s) only and do not necessarily reflect those of the European Union or European Research Executive Agency (REA). Neither the European Union nor the granting authority can be held responsible for them.

Declaration of competing interest

The authors declare that they have no known competing financial interests or personal relationships that could have appeared to influence the work reported in this paper.

Acknowledgments

The authors acknowledge the support of the European Research Executive Agency (REA) for funding this research under the project "ENPOWER-Enhancing Scientific Capacity for Energy Poverty (101160253-ENPOWER-HORIZON-WIDERA-2023-ACCESS-02)".

Also, this research was supported by the Science Fund of the Republic of Serbia, #GRANT No 4344, Forward-Looking Framework for Accelerating Households' Green Energy Transition - FF GreEN and by the Ministry of Science, Technological Development and Innovation of the Republic of Serbia, Contract No. 451-03-137/2025-03/200105, Mechanical Faculty, University of Belgrade.

Data availability

Data will be made available on request.

References

[1] Herrando M, Wang K, Huang G, Otanicar T, Mousa OB, Agathokleous RA, et al. A review of solar hybrid photovoltaic-thermal (PV-T) collectors and systems. Prog Energy Combust Sci 2023;97:101072. https://doi.org/10.1016/j.pecs.2023.101072.

[2] Renewables 2023 - analysis and forecast to 2028. International Energy Agency (IEA); 2024. https://www.iea.org/reports/renewables-2023. [Accessed 22 October 2025].

[3] Gallardo-Saavedra S, Karlsson B. Simulation, validation and analysis of shading effects on a PV system. Sol Energy 2018;170:828–39. https://doi.org/10.1016/j.solener.2018.06.035.

[4] Nezamisavojbolaghi M, Davodian E, Bouich A, Tlemçani M, Mesbahi O, Janeiro FN. The impact of dust deposition on PV panels' efficiency and mitigation solutions. Energies 2023;16:2–19. https://doi.org/10.3390/en16248022.

[5] Conceição R, González-Aguilar J, Merrouni AA, Romero M. Soiling effect in solar energy conversion systems: a review. Renew Sustain Energy Rev 2022;162:112434. https://doi.org/10.1016/j.rser.2022.112434.

[6] Korab R, Połomski M, Naczyński T, Kandzia T. A dynamic thermal model for a photovoltaic panel under varying atmospheric conditions. Energy Convers Manag 2023;280:116773. https://doi.org/10.1016/j.enconman.2023.116773.

[7] Shadid R, Khawaja Y, Bani-Abdullah A, Akho-Zahieh M, Allahham A. Investigation of weather conditions on the output power of various photovoltaic systems. Renew Energy 2023;217:119202. https://doi.org/10.1016/j.renene.2023.119202.

[8] Fouad MM, Shihata LA, Morgan EI. An integrated review of factors influencing the performance of photovoltaic panels. Renew Sustain Energy Rev 2017;80:1499–511. https://doi.org/10.1016/j.rser.2017.05.141.

[9] Yuan W, Li JJZ, Zhou F, Ren X, Zhao X, Liu S. Comparison study of the performance of two kinds of photovoltaic/thermal (PV/T) systems and a PV panel at high ambient temperature. Energy 2018;148:1153–61. https://doi.org/10.1016/j.energy.2018.01.121.

[10] Fudholi A, Sopian K, Yazdi MH, Ruslan MH, Ibrahim A, Kazem HA. Performance analysis of photovoltaic thermal (PVT) water collectors. Energy Convers Manag 2014;78:641–51. https://doi.org/10.1016/j.enconman.2013.11.017.

[11] Korkut TB, Gören A, Rachid A. Numerical and experimental study of a PVT water system under daily weather conditions. Energies 2022;15. https://doi.org/10.3390/en15186538.

[12] Santos LO, Carvalho PCM, Filho COC. Photovoltaic cell operating temperature models: a review of correlations and parameters. IEEE J Photovoltaics 2022;12:179–90. https://doi.org/10.1109/JPHOTOV.2021.3113156.

[13] Shaker LM, Al-Amiery AA, Hanoon MM, Al-Azzawi WK, Kadhum AAH. Examining the influence of thermal effects on solar cells: a comprehensive review. Sustain Energy Res 2024;11. https://doi.org/10.1186/s40807-024-00100-8.

[14] Salimi H, Lavasani AM, Ahmadi-Danesh-Ashtiani H, Fazaeli R. Effect of dust concentration, wind speed, and relative humidity on the performance of photovoltaic panels in Tehran. Energy Sources 2023;45:7867–77. https://doi.org/10.1080/15567036.2019.1677811.

[15] Chowdhury M, Shahariar S, Rahman KS, Chowdhury T, Nuthammachot N, Techato K, Akhtaruzzaman M, Tiong SK, Sopian K, Amin N. An overview of solar photovoltaic panels' end-of-life material recycling. Energy Strategy Rev 2020;27:100431. https://doi.org/10.1016/j.esr.2019.100431.

[16] Elbar A, Refat A, Yousef MS, Hassan H. Energy, exergy, exergoeconomic and enviroeconomic (4E) evaluation of a new integration of solar still with photovoltaic panel. J Clean Prod 2019;233:665–80. https://doi.org/10.1016/j.jclepro.2019.06.111.

[17] Lakhdar N, Hima A. Electron transport material effect on performance of perovskite solar cells based on CH3NH3GeI3. Opt Mater 2020;99. https://doi.org/10.1016/j.optmat.2019.109517.

[18] Lee J, Shin J. The economic value of new sustainable products: the case of photovoltaic thermal (PVT) hybrid solar collectors. Energies 2023;16. https://doi.org/10.3390/en16145473.

[19] Santiago I, Trillo-Montero D, Moreno-Garcia IM, Pallares-Lopez V, Luna-Rodríguez JJ. Modeling of photovoltaic cell temperature losses: a review and a practice case in south Spain. Renew Sustain Energy Rev 2018;90:70–89. https://doi.org/10.1016/j.rser.2018.03.054.

[20] Baskaran VK, Chidambaram A, Balachandran GB. Performance analysis of hybrid PV/T systems: exploring synergistic effects of aluminium, copper, and pristine graphene as high-thermal-conductivity materials. Therm Sci Eng Prog 2025;62. https://doi.org/10.1016/j.tsep.2025.103598.

[21] Chiang W, Permanaa I, Wang F, Chen H, Erdenebayar M. Experimental investigation for an innovative hybrid photovoltaic/Thermal (PV/T) solar system. Energy Rep 2022;8:910–8. https://doi.org/10.1016/j.egyr.2022.10.264.

[22] Ouédraogo A, Zouma B, Ouédraogo E, Guissou L, Bathiébo DJ. Individual efficiencies of a polycrystalline silicon PV cell versus temperature. Results Opt 2021;4. https://doi.org/10.1016/j.rio.2021.100101.

[23] Hosouli S, Gomes J, Loris A, Pazmiño IA, Naidoo A, Lennermo G, Mohammadi H. Evaluation of a solar photovoltaic thermal (PVT) system in a dairy farm in Germany. Sol Energy Adv 2023;3. https://doi.org/10.1016/j.seja.2023.100035.

[24] Han H, Kurses M, Harraz A, Xu J. Comparative study of PV, PVT, and solar thermal systems for residential applications in Europe. Energy 2025;336:138368. https://doi.org/10.1016/j.energy.2025.138368.

[25] Vallati A, Di Matteo M, Basso GL, Ocło P, Fiorini CV. Definition of a PVT coupled water source heat pump system through optimization of individual components. Energy 2024;307:132455. https://doi.org/10.1016/j.energy.2024.132455.

[26] Vallati A, Di Matteo M, Sundararajan M, Muzi F, Fiorini CV. Development and optimization of an energy saving strategy for social housing applications by water source-heat pump integrating photovoltaic-thermal panels. Energy 2024;301:131531. https://doi.org/10.1016/j.energy.2024.131531.

[27] Hossain MS, Pandey AK, Selvaraj J, Rahim NA, Rivai A, Tyagi VV. Thermal performance analysis of parallel serpentine flow based photovoltaic/thermal (PV/T) system under composite climate of Malaysia. Appl Therm Eng 2019;153:861–71. https://doi.org/10.1016/j.applthermaleng.2019.01.007.

[28] Satpute J, Srinidhi C, Rathore SS, Yadav SM, Kumar A, Gajbhiye A, et al. Parametric influence and efficiency assessment of water-cooled photovoltaic thermal PV/T heat exchanger designs. Energy 2025;320:135218. https://doi.org/10.1016/j.energy.2025.135218.

[29] Kazem HA. Evaluation and analysis of water-based photovoltaic/thermal (PV/T) system. Case Stud Therm Eng 2019;13. https://doi.org/10.1016/j.csite.2019.100401.

[30] Prabhakar J, Biplab D, Rajat G, Niraj K. An experimental analysis of photovoltaic thermal collector with trapezoidal and plain plates: an energy, exergy, and life cycle assessment. Appl Therm Eng 2025;274. https://doi.org/10.1016/j.applthermaleng.2025.126769.

[31] Yu Y, Yang H, Peng J, Long E. Performance comparisons of two flatplate photovoltaic thermal collectors with different channel configurations. Energy 2019;175:300–8. https://doi.org/10.1016/j.energy.2019.03.054.

[32] Abdullah AL, Misha S, Tamaldin N, Rosli MAM, Sachit FA. Theoretical study and indoor experimental validation of performance of the new photovoltaic thermal solar collector (PVT) based water system. Case Stud Therm Eng 2020;18. https://doi.org/10.1016/j.csite.2020.100595.

[33] Poredoš P, Tomc U, Petelin N, Vidrih B, Flisar U, Kitanovski A. Numerical and experimental investigation of the energy and exergy performance of solar thermal, photovoltaic and photovoltaic-thermal panels based on roll-bond heat exchangers. Energy Convers Manag 2020;210:112674. https://doi.org/10.1016/j.enconman.2020.112674.

[34] Harby K, Attia MEH, Khelifa A, Amin M, Cuce E, Abdelgaied M. Performance characteristics of optimized bi-fluid photovoltaic-thermal solar system: a comparative study of innovative cooling system made of different materials. Appl Therm Eng 2025;278:127283. https://doi.org/10.1016/j.applthermaleng.2025.127283.
[35] Tofael MA, Rashel MR, Islam M, Hoque TT, Tlemçani M, Janeiro FM. Characterization, performance, and efficiency analysis of hybrid photovoltaic thermal (PVT) systems. Energies 2025;18. https://doi.org/10.3390/en18051050.
[36] Alami YE, Ameur A, Benhmida M, Rabhi A, Baghaz E. Performance evaluation of different new channel box photovoltaic thermal systems. J Clean Prod 2024;478:143953. https://doi.org/10.1016/j.jclepro.2024.143953.
[37] Shahsavar A, Prabhakar J, Arici M, Kefayati G. A comparative experimental investigation of energetic and exergetic performances of water/magnetite nanofluid-based photovoltaic/thermal system equipped with finned and unfinned collectors. Energy 2021;220:119714. https://doi.org/10.1016/j.energy.2020.119714.
[38] Prabhakar J, Das B, Gupta R, Mondol JD, Ehyaei MA. Review of recent research on photovoltaic thermal solar collectors. Sol Energy 2023;257:164–95. https://doi.org/10.1016/j.solener.2023.04.004.
[39] Shahsavar A, Prabhakar J, Askari IB. Experimental study of a nanofluid-based photovoltaic/thermal collector equipped with a grooved helical microchannel heat sink. Appl Therm Eng 2022;217:119281. https://doi.org/10.1016/j.applthermaleng.2022.119281.
[40] Energy statistics for 2024. Agency for statistics of Bosnia and Herzegovina. https://bhas.gov.ba/data/Publikacije/Saopstenja/2025/ENE_03_2024_Y1_1_BS.pdf. [Accessed 21 January 2026].
[41] Dubey S, Sarvaiya JN, Seshadri B. Temperature dependent photovoltaic (PV) efficiency and its effect on PV production in the world - a review. Energy Proc 2013;33:311–21. https://doi.org/10.1016/j.egypro.2013.05.072.
[42] Ross RG. Interface design considerations for terrestrial solar cells panels. In: Proceedings of the 12th IEEE photovoltaic specialists conference; 1976.
[43] Lasnier F, Ang TG. Photovoltaic engineering handbook. New York: Taylor & Francis; 1990.
[44] King DL, Boyson WE, Kratochvill JA. Photovoltaic array performance model. Sandia National Laboratories; 2004. https://doi.org/10.2172/919131.
[45] Skoplaki E, Boudouvis AG, Palyvos JA. A simple correlation for the operating temperature of photovoltaic panels of arbitrary mounting. Sol Energy Mater Sol Cells 2008;92:1393–402. https://doi.org/10.1016/j.solmat.2008.05.016.
[46] Kamuyu CLW, Lim JR, Won CS, Ahn HK. Prediction model of photovoltaic panel temperature for power performance of floating PVs. Energies 2018;11. https://doi.org/10.3390/en11020447.
[47] Zouine M. Mathematical models calculating PV Panel temperature using weather data: experimental study. In: Proceedings of the 1st international conference on electronic engineering and renewable energy. ICEERE. Singapore: Springer; 2018. https://doi.org/10.1007/978-981-13-1405-6_72.
[48] Evans DL. Simplified method for predicting photovoltaic array output. Sol Energy 1981;27:555–60. https://doi.org/10.1016/0038-092X(81)90051-7.
[49] Skoplaki E, Palyvos JA. On the temperature dependence of photovoltaic panel electrical performance: a review of efficiency/power correlations. Sol Energy 2009;83:614–24. https://doi.org/10.1016/j.solener.2008.10.008.
[50] Notton G, Cristofari C, Mattei M, Poggi P. Modelling of a double-glass photovoltaic panel using finite differences. Appl Therm Eng 2005;25:2854–77. https://doi.org/10.1016/j.applthermaleng.2005.02.008.
[51] Limane B, Ould-Lahoucine C, Diaf S. Modeling and simulation of the thermal behavior and electrical performance of PV panels under different environment and operating conditions. Renew Energy 2023;219:119420. https://doi.org/10.1016/j.renene.2023.119420.
[52] Arnesson H, Olympios AV, Harraz AA, Xu J. Comprehensive energy, economic, and environmental analysis of a hybrid photovoltaic–thermal (PVT) heat pump system. Energy 2025;331:136563. https://doi.org/10.1016/j.energy.2025.136563.
[53] Tofael MA, Rashel MR, Wadud MAA, Hoque TT, Janeiro FM, Tlemçani M. Mathematical modeling, parameters effect, and sensitivity analysis of a hybrid PVT system. Energies 2024;17. https://doi.org/10.3390/en17122887.
[54] Han Z, Liu K, Li G, Zhao X, Shittu S. Electrical and thermal performance comparison between PVT-ST and PV-ST systems. Energy 2021;237:121589. https://doi.org/10.1016/j.energy.2021.121589.
[55] Farulla GA, Cellura M, Guarino F, Ferraro M. A review of thermochemical energy storage systems for power grid support. Appl Sci 2020;10. https://doi.org/10.3390/app10093142.
[56] Islam MP, Morimoto T. Advances in low to medium temperature non-concentrating solar thermal technology. Renew Sustain Energy Rev 2018;82:2066–93. https://doi.org/10.1016/j.rser.2017.08.030.
[57] Kardaš Ančić D, Komatina M, Gvero P. Photovoltaic panel temperature estimation under various environmental conditions: preliminary experimental and theoretic study. Therm Sci 2025;29:3367–76. https://doi.org/10.2298/TSCI241224049K.